RECONSTRUCTING THE TRANSITION RATE FUNCTION OF A BROADWELL RANDOM WALK FROM EXIT TIMES[*]

QUNHUI HAN[†] AND PAK-WING FOK[†]

Abstract. In this paper, we utilize the layer stripping method, a method used in seismology by geophysicists, to study a stochastic inverse problem arising from a one-dimensional Broadwell process. The Broadwell process can be described as a random walk of a particle that transitions, with a spatially dependent flip rate, between two states associated with the same speed but with different signs of velocities. Our goal is to reconstruct the spatially dependent flip rate function of a one-dimensional Broadwell process from exit time distributions out of a finite interval. In principle, we are able to reconstruct flip rate functions with error within $O(10^{-2})$ from $O(10^5)$ exit times when the particle speed is unity. For smaller particle speeds, the noise increases for a fixed number of exit times. This method is less time consuming compared with traditional projection methods which involve optimization.

Key words. random walk, inverse problem, Broadwell, layer stripping algorithm

AMS subject classifications. 60G40, 93E10, 92-08

DOI. 10.1137/130927954

1. Introduction. A one-dimensional Broadwell process [7, 8, 12, 21, 26] can be described as a particle's persistent random walk within a finite interval, where the particle transitions, with a given flip rate, between two states having the same speed but opposite directions. The time it takes for the particle to first reach either endpoints of the interval is recorded as the exit time. Broadwell phenomena are ubiquitous in a wide range of areas, such as bacteria chemotaxis [35], microtubule growth [6], optical tomography [3], charge transport in DNA [15], and interactions of individuals among fish schools [13]. There are many cases where researchers would like to infer parameters of a random walk from first exit times [14, 16, 27]. Problems of this type are essentially stochastic inverse problems.

One application of stochastic inverse problems arises in the context of neuroscience. In the mammalian central nervous system [19, 34], the voltage between the interior and the exterior of a neuron's membrane fluctuates as a result of the noisy synaptic inputs from other neurons. This fluctuating voltage can be described as a random walk. Once the voltage reaches a limit, it spikes and resets to zero. The interspike time defines the voltage's first passage time [28], the time that a random walk first reaches a specified value. Thus the stochastic inverse problem of interest is to infer the intrinsic current-voltage relationship of the neuron [33] from the first passage time distribution of the voltage. A second application of the inverse stochastic problem arises from diffuse optical tomography [3], where the underlying stochastic process may be modeled as diffusive motion. However, a sequence of studies [5, 14] shows that the inverse problem associated with diffusive motion is ill-posed, and the related existence and uniqueness of the spatially dependent parameters are not well established. This triggers our interest to study stochastic problems of other types of random walk.

Many well-established optimization theories and numerical methods have been used to address the ill-posed issue of inverse problems, such as the minimization of a Tikhonov regularized objective function. However, it might be time consuming to optimize an objective function due to the large number of iterations. Geophysicists have developed the layer stripping algorithm (or downward continuation algorithm) [10, 20] as an alternative to solving an optimization problem. The layer stripping algorithm, which arises from one-dimensional inverse scattering (impulse-response) problem in reflection seismology [10], speech synthesis [31], and transmission-line models [9], is established on the method of characteristics [30], the finite difference method, and causal boundary data. Another classical inversion method commonly used is formulated in the form of an integral equation and noncausal boundary data. Boundary data is causal if it is zero when time is negative; the boundary data is noncausal if it is nonzero when time is negative. There are various integral equations proposed by Krein [25], Gopinath and Sondhi [22, 23], Gelfand and Levitan [18, 11], and Agranovich, Marchenko, and Seckler [1]. These integral equations, which are associated with special structured kernels, such as Toeplitz [24] and Hankel [29], are formulated by considering particular impulse-response pairs of scattering data measured at the boundary of the medium. The difference between the layer stripping algorithm and the method of integral equations is that the layer stripping algorithm utilizes the differential structure and the causality of propagation to reconstruct the medium layer by layer, while the integral equation utilizes the causality, symmetry, and losslessness properties of the medium for reconstruction.

In this paper, we generalize the study of diffusive processes to Broadwell processes [7, 8, 12, 21], which are governed by the telegrapher's equation [26]. The particle switches between the two states with a given flip rate. The transition time between the two states is shorter if the flip rate is larger. This property indicates that in the limit of large flip rate, the Broadwell process behaves like a diffusive motion [6, 15]. Hence, we may obtain a more intuitive and deeper understanding of the inverse diffusion problem by studying the inverse Broadwell problem. In this paper, we only study the Broadwell process with constant speed and spatially dependent flip rate. We also define the exit time as the travel time needed for the particle starting from one endpoint of a finite interval to exit from either endpoint. The exit time distribution yields the causal boundary data, from which we are able to reconstruct flip rate function using the layer stripping algorithm.

The layer stripping algorithm is distinct from the projection method used in our previous paper [16] both in terms of the underlying mathematics and conditions for the method to be applicable. The layer stripping algorithm relies on the structure of the PDE (most notably, its hyperbolicity), while the projection method reconstructs the flip rate function by minimizing an objective function that stems from solving the forward problem. Note that optimization can always be used for inverse problems, but usually lead to ill-posed problems. As for the conditions, the layer stripping method reconstructs flip rate functions that are bounded on the finite interval of interest and even discontinuous flip rate functions can be reconstructed without any additional difficulty. In contrast, the projection method requires that the flip rate function is known a priori to be a low degree polynomial. On the other hand, the data for the layer stripping algorithm must come from a Broadwell process that starts from either endpoint of the interval, while the data for the projection method is generated by starting a Broadwell process at a position strictly inside the interval.

This paper is organized as follows. In section 2, we give a detailed description of a two-state Broadwell process and restrict our study to the case with a constant speed
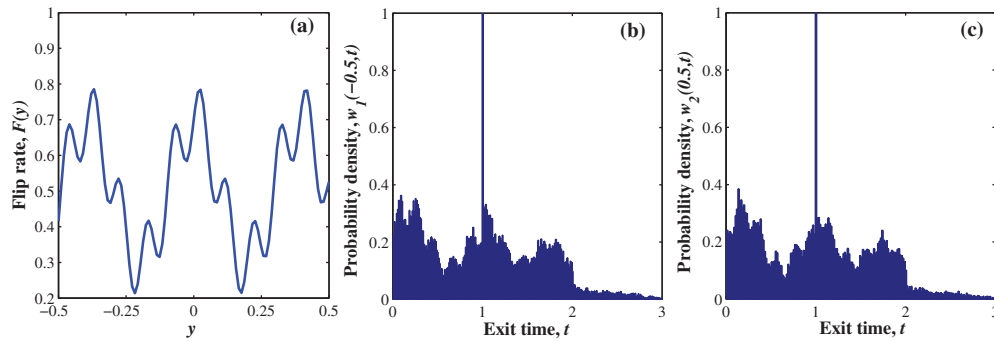
FIG. 1. *Simulated exit time distributions of a Broadwell process with flip rate $F(y) = 0.5 +$ $0.2\cos(16y) + 0.1\sin(64y)$, constant velocity $v = 1$, and $L = 1$. (a) The flip rate function $F(y)$. (b) Exit time distribution w_1 starting from $x = -0.5$ with velocity $+v$, generated by $F(y)$ in (a). (c) Exit time distribution w_2 starting from $x = 0.5$ with velocity $-v$, generated by flip rate $F(y)$ in (a). The number of exit times to generate each distribution is $M = 10^5$.*

and spatially dependent flip rate. We then derive the Kolmogorov backward equation for the Broadwell process and state both the forward problem and inverse problem. In section 3, we discuss the numerical scheme for our work. We implement the layer stripping algorithm to reconstruct the flip rate functions. In section 4, we present our results of reconstruction obtained from simulated data and the convergence rate of the layer stripping algorithm. In section 5, we summarize our findings.

2. Two-state Broadwell model and statement of inverse problem. The two-state Broadwell model can be described as a particle's random walk parameterized by a starting position $x \in [-L/2, L/2]$, a velocity $+v$ (state 1, where v is a positive constant) or $-v$ (state 2), and a flip rate $F(y)$, where $y \in [-L/2, L/2]$ represents the current position at time σ. While traveling with speed v, the particle shifts between the two states with probability $F(y)d\sigma$ within time interval $(\sigma, \sigma + d\sigma)$.

When the particle exits from either endpoint, the total travel time is recorded. If the Broadwell process is repeated a large number of times, we obtain the exit time distribution $w_1(x, t)$ if the particle initially starts from x in state 1 and $w_2(x, t)$ if the particle initially starts from x in state 2, where t is the exit time. Figure 1 shows the simulated exit time distributions $w_1(-L/2, t)$ and $w_2(L/2, t)$ of a Broadwell process with a given flip rate function $F(y)$. Then the exit time distributions follow the equations:

$$(2.1) \qquad \frac{\partial w_1}{\partial t} - v\frac{\partial w_1}{\partial x} = F(x)(w_2 - w_1),$$

$$(2.2) \qquad \frac{\partial w_2}{\partial t} + v\frac{\partial w_2}{\partial x} = F(x)(w_1 - w_2),$$

$$(2.3) \qquad w_1(L/2, t) = \delta(t),$$

$$(2.4) \qquad w_2(-L/2, t) = \delta(t)$$

for $t > 0$, and

$$(2.5) \qquad w_1(x, t) = 0,$$

$$(2.6) \qquad w_2(x, t) = 0$$

for $t \leq 0$, where $\delta(t)$ is the Dirac delta function. A complete derivation of the

Kolmogorov backward equation for the exit time distribution of a two-state Broadwell process can be found in Appendix A.

The forward problem is to solve (2.1)–(2.6) for exit time distributions $w_1(x,t)$ and $w_2(x,t)$, $-L/2 < x < L/2$, and $t > 0$, given starting position x, flip rate $F(y)$, and velocity $\pm v$. Therefore, in Figure 1, the forward problem is that given Figure (a), we want to generate plots (b) and (c). However, in this paper, we are more interested in the inverse problem.

Inverse problem statement. Consider (2.1)–(2.6). Given velocities $\pm v$ and exit time distributions at the boundaries $x = \pm L/2$: $w_1(-L/2,t)$ and $w_2(L/2,t)$, $t > 0$, reconstruct the flip rate $F(x) \in C(-L/2, L/2)$.

To illustrate the problem, given Figures 1(b) and (c), we want to reconstruct $F(y)$ in Figure 1(a). Notice that Figures 1(b) and (c) contain "spikes." The spike is a numerical approximation of a Dirac delta function, which corresponds to an immediate particle exit at time $t = L/v$. For more details, see [16].

3. Reconstruction algorithm. For reconstruction, we use two types of exit time distribution. One comes from the solution of the forward problem (perfect data), and the other one comes from directly simulating a Broadwell process (noisy data); details can be found in [16]. In this section, we give details on solving the forward problem and then discuss the layer stripping method to solve the inverse problem.

3.1. Solution to the forward problem.

3.1.1. Propagation of singularities. We break up the forward problem into two subproblems. First consider

$$(3.1) \qquad \frac{\partial w_1}{\partial t} - v\frac{\partial w_1}{\partial x} = F(x)(w_2 - w_1),$$

$$(3.2) \qquad \frac{\partial w_2}{\partial t} + v\frac{\partial w_2}{\partial x} = F(x)(w_1 - w_2),$$

$$(3.3) \qquad w_1(L/2, t) = 0,$$

$$(3.4) \qquad w_2(-L/2, t) = \delta(t).$$

Let H be the Heaviside function, we look for a solution in the form

$$(3.5) \qquad w_1(x,t) = a_0(x,t)\delta(\xi) + a_1(x,t)H(\xi),$$

$$(3.6) \qquad w_2(x,t) = b_0(x,t)\delta(\xi) + b_1(x,t)H(\xi),$$

where a_0, a_1, b_0, b_1 are differentiable functions and $\xi = t - x/v - L/(2v)$. Substituting (3.5)–(3.6) into (3.1)–(3.2), we have

$$2a_0\delta'(\xi) + \left[\frac{\partial a_0}{\partial t} - v\frac{\partial a_0}{\partial x} + 2a_1 - F(b_0 - a_0)\right]\delta(\xi)$$

$$+ \left[\frac{\partial a_1}{\partial t} - v\frac{\partial a_1}{\partial x} - F(b_1 - a_1)\right]H(\xi) = 0,$$

$$\left[\frac{\partial b_0}{\partial t} + v\frac{\partial b_0}{\partial x} - F(a_0 - b_0)\right]\delta(\xi) + \left[\frac{\partial b_1}{\partial t} + v\frac{\partial b_1}{\partial x} - F(a_1 - b_1)\right]H(\xi) = 0,$$

from which we match the coefficients of $\delta'(\xi)$ and $\delta(\xi)$, and deduce that on $\xi = 0$,

(3.7)
$$a_0 \delta'(\xi) = 0,$$

$$2a_1 = F(b_0 - a_0) - \frac{\partial a_0}{\partial t} + v \frac{\partial a_0}{\partial x},$$

(3.8)
$$\frac{\partial b_0}{\partial t} + v \frac{\partial b_0}{\partial x} = F(a_0 - b_0).$$

We shall see in the Appendix B that (3.7) implies

(3.9)
$$a_0 = 0 \quad \text{on } \xi = 0,$$

(3.10)
$$\frac{\partial a_0}{\partial t} - v \frac{\partial a_0}{\partial x} = 0 \quad \text{on } \xi = 0.$$

Substituting (3.9)–(3.10) into (3.7)–(3.8), we have that when $\xi = 0$, $a_0(x) = 0$, $b_0(x) = \exp[-\int_{-L/2}^{x} \frac{F(x')}{v} \, dx']$, and

(3.11)
$$a_1(x, t) = a_1(x) = \frac{F(x)}{2} \exp\left[-\int_{-L/2}^{x} \frac{F(x')}{v} dx' \right].$$

We also match the coefficients of $H(\xi)$, so that when $\xi > 0$,

(3.12)
$$\frac{\partial a_1}{\partial t} - v \frac{\partial a_1}{\partial x} = F(x)(b_1 - a_1),$$

(3.13)
$$\frac{\partial b_1}{\partial t} + v \frac{\partial b_1}{\partial x} = F(x)(a_1 - b_1).$$

We solve (3.12)–(3.13) in the triangular domain $x > -L/2$, $t - x/v - L/(2v) > 0$, $t < L/(2v)$ with boundary conditions (3.11) and

(3.14)
$$b_1(-L/2, t) = 0,$$

which comes from setting $x = -L/2$ in (3.6) and comparing with (3.4). Note that, because in the hyperbolic system the wave moves in a one-dimensional medium with speed v, a disturbance at $x = -L/2$, $t = 0$ can have no "effect" at x until $t > x/v + L/(2v)$, so we have $b_1(x, t) = a_1(x, t) \equiv 0$ in the region $x < L/2$, $t - x/v - L/(2v) < 0$, $t > 0$. See subplot (a) of Figure 2.

Similarly, we look for a solution to the second subproblem

$$\frac{\partial w_1}{\partial t} - v \frac{\partial w_1}{\partial x} = F(x)(w_2 - w_1),$$

$$\frac{\partial w_2}{\partial t} + v \frac{\partial w_2}{\partial x} = F(x)(w_1 - w_2),$$

(3.15)
$$w_1(L/2, t) = \delta(t),$$

$$w_2(-L/2, t) = 0$$

in the form

(3.16)
$$w_1(x, t) = c_0(x, t)\delta(\eta) + c_1(x, t)H(\eta),$$

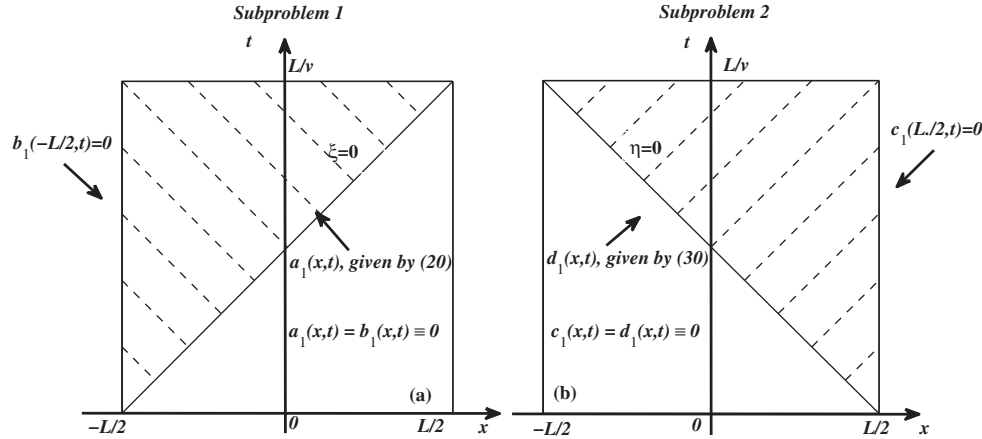$$w_2(x, t) = d_0(x, t)\delta(\eta) + d_1(x, t)H(\eta),$$

FIG. 2. (a) *Singularity structure of* (3.11)–(3.14). (b) *Singularity structure of* (3.17)–(3.20).

where $\eta = t + x/v - L/(2v)$. After some similar calculations, we have that when $\eta = 0$, $d_0(x,t) = 0$, $c_0(x,t) = \exp[- \int_x^{L/2} \frac{F(x')}{v} dx']$, and

$$(3.17) \qquad d_1(x,t) = \frac{F(x)}{2} \exp\left[- \int_x^{L/2} \frac{F(x')}{v} dx' \right].$$

We also have that when $\eta > 0$,

$$(3.18) \qquad \frac{\partial c_1}{\partial t} - v\frac{\partial c_1}{\partial x} = F(x)(d_1 - c_1),$$

$$(3.19) \qquad \frac{\partial d_1}{\partial t} + v\frac{\partial d_1}{\partial x} = F(x)(c_1 - d_1).$$

We solve (3.18)–(3.19) in the triangular domain $x < L/2$, $t + x/v - L/(2v) > 0$, $t < L/(2v)$ with boundary conditions (3.17) and

$$(3.20) \qquad c_1(L/2, t) = 0,$$

which comes from setting $x = L/2$ in (3.16) and comparing with (3.15). Note that, because in the hyperbolic system the wave moves in a one-dimensional medium with speed v, a disturbance at $x = L/2$, $t = 0$ can have no "effect" at x until $t > -x/v + L/(2v)$, so we have $c_1(x,t) = d_1(x,t) \equiv 0$ in the region $x < L/2$, $t + x/v - L/(2v) < 0$, $t > 0$. See subplot (b) of Figure 2. In fact, we can solve (3.18)–(3.19) by noting the following steps: (i) let $x \to -x$ in (3.17)–(3.20); (ii) let $\widetilde{c_1}(x,t) = c_1(-x,t)$ and $\widetilde{d_1}(x,t) = d_1(-x,t)$. Then (3.17)–(3.20) become

$$(3.21) \qquad \frac{\partial \widetilde{c_1}}{\partial t} + v\frac{\partial \widetilde{c_1}}{\partial x} = F(-x)(\widetilde{d_1} - \widetilde{c_1}),$$

$$\frac{\partial \widetilde{d_1}}{\partial t} - v\frac{\partial \widetilde{d_1}}{\partial x} = F(-x)(\widetilde{c_1} - \widetilde{d_1}),$$

$$\widetilde{c_1}(-L/2, t) = 0,$$

$$(3.22) \qquad \widetilde{d_1}(x,t) = \frac{F(-x)}{2} \exp\left[- \int_{-L/2}^{x} \frac{F(-y)}{v} dy \right]$$

$$\text{on} \quad t = x/v + L/(2v),$$

which are exactly the same as (3.11)–(3.14) except $F(x)$ is replaced by $F(-x)$. This symmetry is used to quickly generate solutions to the full problem (2.1)–(2.6), whose solution arises from a superposition of the subproblem solutions and can be represented as

$$(3.23) \qquad w_1(x,t) = a_1(x,t)H(\xi) + c_0(x,t)\delta(\eta) + \widetilde{c_1}(-x,t)H(\eta),$$

$$(3.24) \qquad w_2(x,t) = b_0(x,t)\delta(\xi) + b_1(x,t)H(\xi) + \widetilde{d_1}(-x,t)H(\eta).$$

In Appendix C, we give a numerical algorithm to generate the perfect data of the exit time distributions $w_1(-L/2,t)$ and $w_2(L/2,t)$. We could also generate noisy data $w_1(-L/2,t)$ and $w_2(L/2,t)$ by simulating a Broadwell random walk using a Monte Carlo method which is based on a rejection-acceptance algorithm [4]. A full description of our Monte Carlo simulation is presented in our previous paper [16]. Once $w_1(-L/2,t)$, $w_2(L/2,t)$ are calculated, we are able to find the corresponding cumulative distribution functions:

$$W_1(-L/2,t) = \int_0^t w_1(-L/v,t')\mathrm{d}t' \equiv h_1(t),$$

$$W_2(L/2,t) = \int_0^t w_2(L/v,t')\mathrm{d}t' \equiv h_2(t),$$

which will be used for flip rate reconstruction in section 3.2.

3.1.2. Relationship between $F(x)$ and $w_{1,2}$ along $t = \frac{L}{2v} \pm \frac{x}{v}$. In this section, we derive the relationship between $F(x)$ and $w_{1,2}$ along $t = \frac{L}{2v} \pm \frac{x}{v}$ using (3.23) and (3.24).

Assume $-L/2 \le x \le 0$. Defining $w_1(x, [\frac{x}{v} + \frac{L}{2v}]^+)$ as $U_1(x)$, we have

$$U_1(x) \equiv w_1\left(x, \left[\frac{x}{v} + \frac{L}{2v}\right]^+\right) = a_1\left(x, \left[\frac{x}{v} + \frac{L}{2v}\right]^+\right),$$

$$= \frac{F(x)}{2}\exp\left[-\int_{-L/2}^x \frac{F(x')}{v}\mathrm{d}x'\right],$$

$$= -\frac{v}{2}\frac{\mathrm{d}}{\mathrm{d}x}\exp\left[-\int_{-L/2}^x \frac{F(x')}{v}\mathrm{d}x'\right],$$

$$(3.25) \qquad \Rightarrow F(x) = \frac{2U_1(x)}{1 - 2\int_{-L/2}^x \frac{U_1(x')}{v}\mathrm{d}x'},$$

$$(3.26) \qquad \Rightarrow F(-L/2) = 2U_1(-L/2).$$

Now assume $0 \le x \le L/2$. Similarly, define $w_2(x, [\frac{L}{2v} - \frac{x}{v}]^+)$ as $U_2(x)$. A similar calculation yields

$$(3.27) \qquad F(x) = \frac{2U_2(x)}{1 - 2\int_x^{L/2} \frac{U_2(x')}{v}\mathrm{d}x'},$$

$$(3.28) \qquad \Rightarrow F(L/2) = 2U_2(L/2).$$

Equations (3.25)–(3.28) are the cornerstones of our numerical method for recovery of $F(x)$.

3.2. Layer stripping algorithm to solve inverse problem. We now describe our algorithm for resconstructing the flip rate function $F(x)$ from the exit time distributions $w_1(-L/2, t)$ and $w_2(L/2, t)$. These distributions come from either the solution of the forward problem or a Broadwell process simulation.

We rewrite (2.1)–(2.4) in terms of cumulative distribution functions $W_1(x, t)$ and $W_2(x, t)$:

$$\text{(3.29)} \qquad \frac{\partial W_1}{\partial t} - v\frac{\partial W_1}{\partial x} = F(x)(W_2 - W_1),$$

$$\text{(3.30)} \qquad \frac{\partial W_2}{\partial t} + v\frac{\partial W_2}{\partial x} = F(x)(W_1 - W_2),$$

$$W_1(L/2, t) = H(t),$$

$$W_2(-L/2, t) = H(t),$$

where $H(t)$ is Heaviside function. Then our inverse problem becomes the following: given exit time distribution data $W_1(-L/2, t) \equiv h_1(t)$, $W_2(L/2, t) \equiv h_2(t)$, recover $F(x)$.

To reconstruct $F(x)$, first we use the method of characteristics to rewrite (3.29) and (3.30) as

$$\text{(3.31)} \qquad \frac{dW_1}{dx} = \frac{F(x)}{v}(W_1 - W_2) \quad \text{along } \frac{x}{v} + t = \text{constant},$$

$$\text{(3.32)} \qquad \frac{dW_2}{dx} = \frac{F(x)}{v}(W_1 - W_2) \quad \text{along } \frac{x}{v} - t = \text{constant}.$$

Let $W_1^{(j,i)} = W_1(x_j, t_i)$ and $W_2^{(j,i)} = W_2(x_j, t_i)$, $U_{1,j} = U_1(x_j) = w_1(x_j, t_j)$, $U_{2,j} = U_2(x_j) = w_2(x_j, t_j)$, and $F_j = F(x_j)$, where $x_j = j\Delta x$, $t_i = i\Delta t$, $\Delta x = L/(2N)$, $\Delta t = L/(vN)$.

We present both first order and second order numerical methods to reconstruct flip rate function $F(x)$.

3.2.1. First order layer stripping algorithm. The first order method is realized by using the simple Euler method to solve the ODEs and the rectangle rule to integrate numerically. First, we rewrite (3.31) and (3.32) as

$$\text{(3.33)} \qquad W_1^{(j,i)} = W_1^{(j-1,i+1)} + F_{j-1}\left(W_1^{(j-1,i+1)} - W_2^{(j-1,i+1)}\right)\Delta x/v,$$

$$\text{(3.34)} \qquad W_2^{(j,i)} = W_2^{(j-1,i-1)} + F_{j-1}\left(W_1^{(j-1,i-1)} - W_2^{(j-1,i-1)}\right)\Delta x/v.$$

The finite difference stencils for (3.33) and (3.34) are indicated in Figure 3.

Note that we have the values of $W_1(x_0, t_i) = h_1(t_i)$, $W_2(x_0, t_i) = H(t_i)$, $W_1(x_N, t_i) = H(t_i)$, and $W_2(x_N, t_i) = h_2(t_i)$ for all $i = 0, 1, 2, \ldots, N - 1$, as well as $h_1(t_N) = \lim_{t \to t_N^-} W_1(x_0, t)$ and $h_2(t_N) = \lim_{t \to t_N^-} W_1(x_0, t)$. When $-L/2 \leq x \leq 0$ and N is even, the first order layer stripping algorithm to find $F(x)$ is as follows:

1. Use boundary data $h_1(t_i)$ and $H(t_i)$, (3.25), and (3.26) to compute $U_1(x_0)$, $F(x_0)$:

$$U_{1,0} = U_1(x_0) = w_1(x_0, t_0) = w_1^{(0,0)} = \frac{W_1^{(0,1)} - W_1^{(0,0)}}{\Delta t},$$
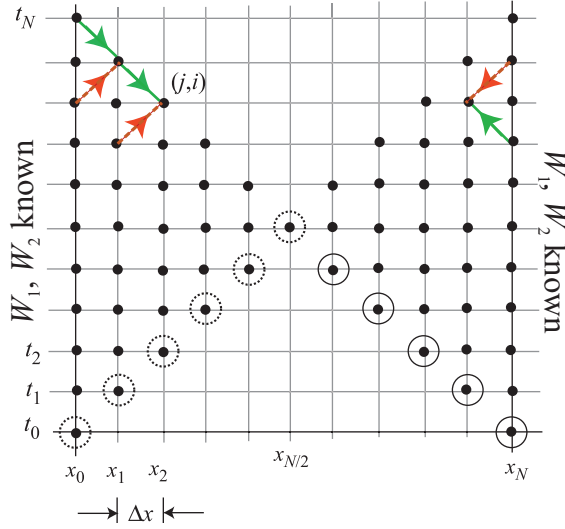
$$F_0 = F(x_0) = 2U_1(x_0).$$

FIG. 3. *Layer stripping algorithm. Dashed circles are values of* $W_1(x, [\frac{x}{v} + \frac{L}{2v}]^+) \equiv U_1(x)$. *Solid circles are values of* $W_2(x, [\frac{L}{2v} - \frac{x}{v}]^+) \equiv U_2(x)$. $W_1^{(j,i)}$ *and* $W_2^{(j,i)}$ *are updated along solid and dashed arrows, respectively.*

2. At each layer $x = x_j$, $j = 1, \ldots, \frac{N}{2} - 1$, we use (3.31), (3.32), (3.25), and (3.27) to calculate the values of $W_1(x_j, t_i)$, $W_2(x_j, t_i)$, $U_1(x_j)$, and $F(x_j)$ for $i = j, j+1, \ldots, N-j-1$, respectively:

$$W_1^{(j,i)} = W_1^{(j-1,i+1)} + F_{j-1}\left(W_1^{(j-1,i+1)} - W_2^{(j-1,i+1)}\right)\frac{\Delta x}{v},$$

$$W_2^{(j,i)} = W_2^{(j-1,i-1)} + F_{j-1}\left(W_1^{(j-1,i-1)} - W_2^{(j-1,i-1)}\right)\frac{\Delta x}{v},$$

$$U_{1,j} = w_1^{(j,j)} = \frac{W_1^{(j,j+1)} - W_1^{(j,j)}}{\Delta t},$$

$$F_j = \frac{2U_{1,j}}{1 - 2(U_{1,0} + \cdots + U_{1,j-1})\Delta x/v}.$$

A similar procedure can be repeated for the right triangle to find $F(x_j)$ when $j = \frac{N}{2}+1, \frac{N}{2}+2, \ldots, N$, given boundary data $h_2(t)$ and $H(t)$. We use linear interpolation to find $F(x_{N/2})$.

3.2.2. Second order layer stripping algorithm. The second order layer stripping algorithm is developed by replacing the simple Euler method and rectangle rule in section 3.2.1 by the predictor-corrector method and trapezoid rule, respectively.

When $-L/2 \le x \le 0$ and N is even, the second order layer stripping algorithm to find $F(x)$ is as follows:

1. Use first order algorithm, boundary data $h_1(t_i)$, and $H(t_i), i = 0, 1, \ldots, N$, where $h_1(t_N) = \lim_{t \to t_N^-} W_1(x_0, t)$, as well as (3.25) and (3.26) to predict $U_1(x_0)$, $F(x_0)$, which are written as $\widehat{U}_1(x_0)$, $\widehat{F}(x_0)$:

$$\widehat{U}_{1,0} = \widehat{U}_1(x_0) = \frac{W_1^{(0,1)} - W_1^{(0,0)}}{\Delta t},$$

$$\widehat{F}_0 = \widehat{F}(x_0) = 2\widehat{U}_1(x_0).$$

Then correct $\widehat{U}_1(x_0)$ by second order differentiation:

$$(3.35) \qquad U_{1,0} = U_1(x_0) = \frac{-W_1^{(0,2)} + 4W_1^{(0,1)} - 3W_1^{(0,0)}}{2\Delta t},$$

$$(3.36) \qquad F_0 = F(x_0) = 2U_1(x_0).$$

In practice, since $U_{1,0}$ and F_0 do not depend on $\widehat{U}_{1,0}$ and $\widehat{F}_0$, we just use (3.35) and (3.36) immediately.

2. At each layer $x = x_j$, $j = 1, \ldots, \frac{N}{2} - 1$, we use the first order algorithms in section 3.2.1, (3.31), (3.32), (3.25), and (3.27) to predict the values of $W_1(x_j, t_i)$, $W_2(x_j, t_i)$, $U(x_j)$, and $F(x_j)$, for $i = j, j+1, \ldots, N - j$,

$$\left.\begin{aligned}
\widehat{W}_1^{(j,i)} &= W_1^{(j-1,i+1)} + F_{j-1}\left(W_1^{(j-1,i+1)} - W_2^{(j-1,i+1)}\right)\frac{\Delta x}{v}, \\
\widehat{W}_2^{(j,i)} &= W_2^{(j-1,i-1)} + F_{j-1}\left(W_1^{(j-1,i-1)} - W_2^{(j-1,i-1)}\right)\frac{\Delta x}{v}, \\
\widehat{U}_{1,j} &= \frac{\widehat{W}_1^{(j,j+1)} - \widehat{W}_1^{(j,j)}}{\Delta t}, \\
\widehat{F}_j &= \frac{2\widehat{U}_{1,j}}{1 - 2(\widehat{U}_{1,0} + \cdots + \widehat{U}_{1,j-1})\Delta x/v}.
\end{aligned}\right\} \text{Predictor}$$

Then use the trapezoid rule to correct them:

$$\left.\begin{aligned}
W_1^{(j,i)} &= W_1^{(j-1,i+1)} + \frac{\Delta x}{2v}\left\{F_{j-1}(W_1^{(j-1,i+1)} - W_2^{(j-1,i+1)})\right. \\
&\qquad\qquad\left. + \widehat{F}_j(\widehat{W}_1^{(j,i)} - \widehat{W}_2^{(j,i)})\right\}, \\
W_2^{(j,i)} &= W_2^{(j-1,i-1)} + \frac{\Delta x}{2v}\left\{F_{j-1}(W_1^{(j-1,i-1)} - W_2^{(j-1,i-1)})\right. \\
&\qquad\qquad\left. + \widehat{F}_j(\widehat{W}_1^{(j,i)} - \widehat{W}_2^{(j,i)})\right\}, \\
U_{1,j} &= \frac{-W_1^{(j,j+2)} + 4W_1^{(j,j+1)} - 3W_1^{(j,j)}}{2\Delta t}, \\
F_j &= \frac{2U_{1,j}}{1 - 2(U_{1,0}/2 + U_{1,1} + \cdots + U_{1,j-1} + U_{1,j}/2)\Delta x/v}.
\end{aligned}\right\} \text{Corrector}$$

A similar procedure can be repeated for the right triangle in Figure 3 to find $F(x_j)$ when $j = \frac{N}{2} + 1, \frac{N}{2} + 2, \ldots, N$, given boundary data $h_2(t)$ and $H(t)$. We use linear interpolation to find $F(x_{N/2})$ from $F(x_{N/2-1})$ and $F(x_{N/2+1})$.

4. Results of reconstruction and discussion. We used the layer stripping algorithm discussed in section 3.2 to reconstruct flip rate functions from data generated by simulating a Broadwell random walk using a Monte Carlo method [16]. In the discussion below, the interval length $L = 1$, particle speed $v = 1$, N is the number of subintervals in $[-L/2, L/2]$, and M is the number of exit times used to generate each exit time distribution $w_1(-L/2, t)$, $w_2(L/2, t)$. Hence, the total number of exit times is always $2M$. Also, notice that the layer stripping algorithm we used does not find the value of $F(x)$ at $x = 0$; so it leaves a "hole" in the $F(x)$, which is filled by interpolation.

In Figure 4, we reconstruct both discontinuous and continuous flip rate functions using the first order layer stripping method. The function in Figure 4(a) is a discontinuous function, the function in Figure 4(b) is a combination of trigonometric and
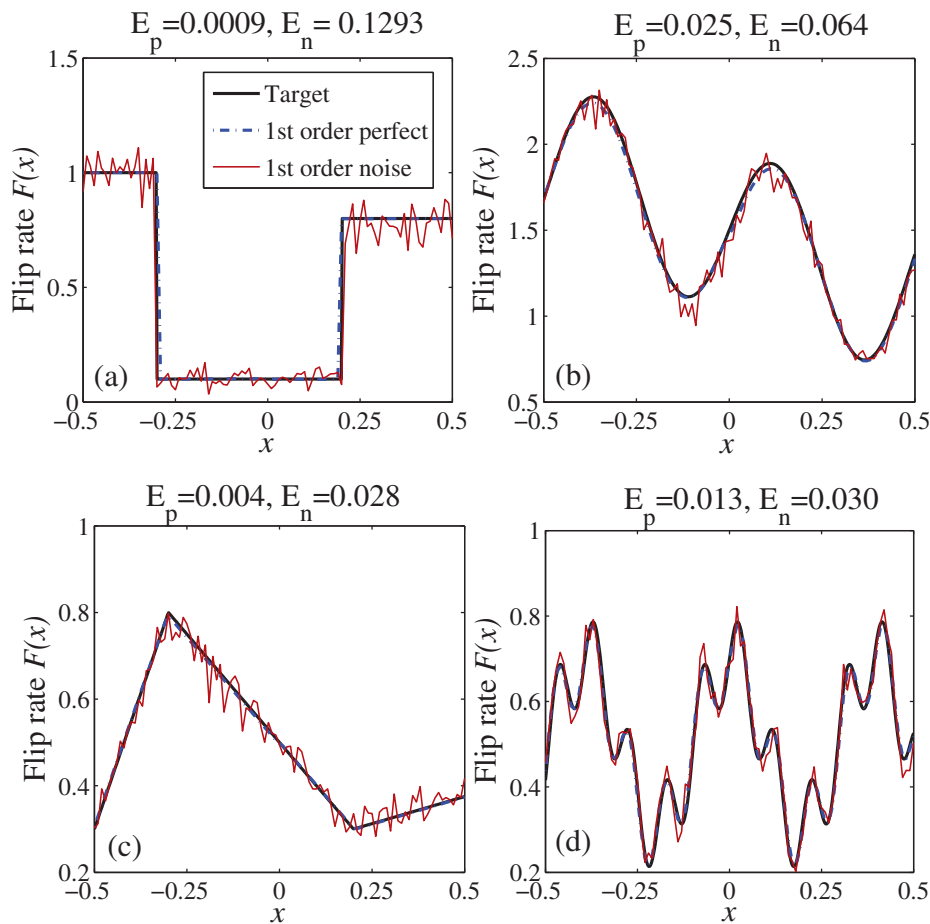
FIG. 4. *Reconstruction of flip rate functions $F(x)$:* (a) $F(x) = 1$ *for* $-0.5 \leq x < -0.3$, $F(x) = 0.1$ *for* $-0.3 \leq x < 0.2$, $F(x) = 0.8$ *for* $-0.2 \leq x \leq 0.5$; (b) $F(x) = \sin(5x)\cos(8x) + \cos(0.3x)\exp(0.5x) + x^2\sin(-0.6x^3) + 0.5$; (c) $F(x) = 2.5x + 1.55$ *for* $-0.5 \leq x \leq -0.3$, $F(x) = -x + 0.5$ *for* $-0.3 < x < 0.2$, $F(x) = 0.25x + 0.25$ *for* $0.2 \leq x \leq 0.5$; (d) $F(x) = 0.5 + 0.2\cos(16x) + 0.1\sin(64x)$, $N = 100$, $M = 200{,}000$.

exponential functions, the function in Figure 4(c) has discontinuous derivatives within $(-L/2, L/2)$, and the function in Figure 4(d) has many extrema within $(-L/2, L/2)$. Let $F(x)$ be the target flip rate function, $F_p(x)$ be the flip rate function reconstructed from perfect data which is generated by solving the forward problem (2.1)–(2.6), and $F_n(x)$ be the flip rate function reconstructed from noisy data which is generated by simulating the Broadwell process. Define the error for perfect data E_p and the error for noisy data E_n in the L^2 norm as

$$E_p = \left(\sum_{i=0}^{N} |F(x_i) - F_p(x_i)|^2 \Delta x \right)^{1/2} \approx \left(\int_{-L/2}^{L/2} |F(x) - F_p(x)|^2 \, dx \right)^{1/2},$$

$$E_n = \left(\sum_{i=0}^{N} |F(x_i) - F_n(x_i)|^2 \Delta x \right)^{1/2} \approx \left(\int_{-L/2}^{L/2} |F(x) - F_n(x)|^2 \, dx \right)^{1/2}.$$

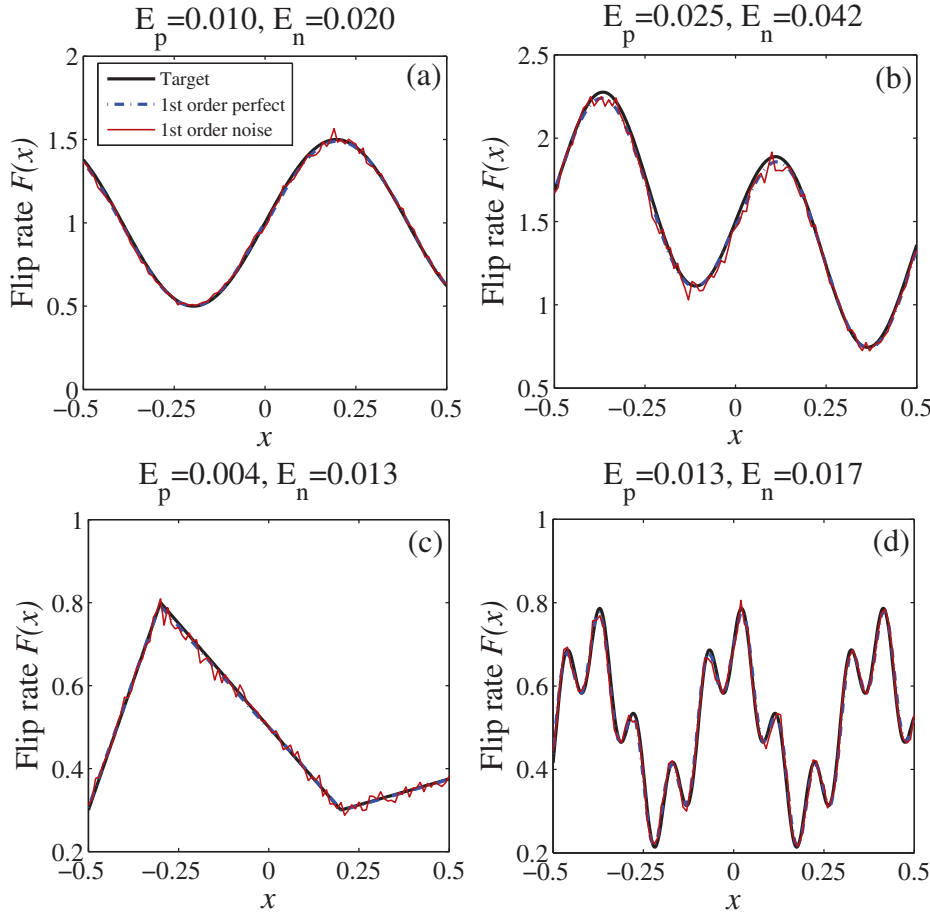In principle, with $N = 100$, we are able to reconstruct any continuous flip rate

FIG. 5. *Reconstruction of flip rate functions $F(x)$:* (a) $F(x) = 0.5\sin(8x) + 1$; (b) $F(x) = \sin(5x)\cos(8x) + \cos(0.3x)\exp(0.5x) + x^2\sin(-0.6x^3) + 0.5$; (c) $F(x) = 2.5x + 1.55$ *for* $-0.5 \le x \le -0.3$, $F(x) = -x + 0.5$ *for* $-0.3 < x < 0.2$, $F(x) = 0.25x + 0.25$ *for* $0.2 \le x \le 0.5$; (d) $F(x) = 0.5 + 0.2\cos(16x) + 0.1\sin(64x)$, $N = 100$, $M = 1{,}000{,}000$.

function with E_p and E_n always within $O(10^{-2})$ given $M = 200{,}000$. The reconstructed curve becomes less noisy, and the accuracy of the flip rate reconstructions from noisy data improves as M increases. For instance, E_n decreases by 30%–50% when $M = 1{,}000{,}000$; see Figures 5(b), (c), and (d). The reconstruction results and errors obtained from first order and second order methods are identical to within three decimal places. Because W_1 and W_2 are noisy, the second order finite difference formula (3.35) is only first order accurate. Hence the accuracy of the predictor-corrector method is first order overall.

We now validate the correct convergence rate of the layer stripping algorithms in section 3.2.1 and 3.2.2, provided that the boundary data for reconstruction is noiseless and corresponds to an actual flip rate function. Assume we are given $0 \le x \le L/2$, $W_2(L/2, t) \equiv h_2(t)$. Let F_N be the reconstructed flip rate function for an $N+1$ point discretization (see Figure 3). Define the error in terms of L^2 norm:

$$E_N = \left(\sum_{i=0}^{N} |F_N(x_i) - F_{6000}(x_i)|^2 \Delta x \right)^{1/2} \approx \left(\int_0^{L/2} |F_N(x) - F_{6000}(x)|^2 \, dx \right)^{1/2},$$
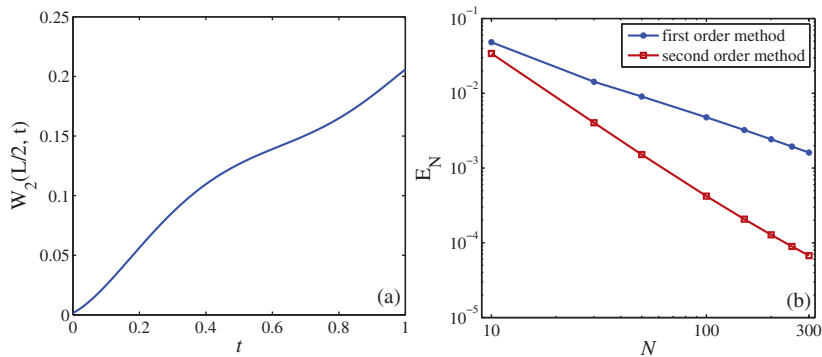
FIG. 6. *Dependence of error in flip rate function $F(x)$ reconstruction on the number of subintervals N. (a) $W_2(L/2, t) \equiv h_2(t) = -0.1403t^6 - 0.7352t^5 + 2.9494t^4 - 3.1707t^3 + 1.1536t^2 + 0.1476t + 0.0015$ for $t \in [0, L/v]$. (b) Given $W_2(L/2, t)$, we use both first and second order layer stripping methods to reconstruct $F(x)$, $0 \le x \le L/2$.*

where we use F_{6000} to approximate the true $F(x)$. In Figure 6, we plot the error E_N against the number of subintervals in $[-L/2, L/2]$. We find that the reconstruction error scales as $O(N^{-1})$ when using the first order algorithm, which agrees with simple Euler and the rectangle rule leading to a first order layer stripping algorithm. The error scales as $O(N^{-2})$ when using second order algorithm, which is consistent with predictor-corrector method and the trapezoid rule leading to a second order layer stripping algorithm.

Our original motivation for studying the Broadwell process was to better understand reconstruction from the exit times of a diffusive motion. In the Broadwell process, the transition distance between the two states is shorter if the flip rate is larger or the velocity is smaller. This property indicates that in the limit of large dimensionless flip rate $\frac{LF(x)}{v}$, the Broadwell process behaves like a diffusive motion. In Figure 7, we reconstruct the flip rate $F(x)$ when v is small from two types of noisy data. In Figures 7(a) and (b) the exit time distribution is generated from Monte Carlo simulation while in Figures 7(c) and (d), the distribution is generated by adding artificial noise that is uniformly distributed on $[-\varepsilon, \varepsilon]$ to $w_{1p}(-L/2, t)$ and $w_{2p}(L/2, t)$ with $\varepsilon = 10^{-5}$.

From Figures 7(a) and (b), we observe that the reconstruction is poor near $x = 0$, because the noise in the probability density functions (PDFs) $w_1(-L/2, t)$ and $w_2(L/2, t)$ for $t \in (0, L/v]$ propagates along characteristics $dx/dt = \pm v$. Our algorithm for reconstructing $F(x)$ accumulates the noise since it requires computing the integral of $w_1(x, [\frac{L}{2v} + \frac{x}{v}]^+)/v$ and $w_2(x, [\frac{L}{2v} - \frac{x}{v}]^+)/v$ through (3.25) and (3.27). This can also be clearly seen in Figure 8, where we reconstruct the flip rate function with values larger at the endpoints than at the midpoint, and v gradually decreases from 1.0 to 0.4.

We use artificial data to reconstruct flip rate functions in Figures 7(c) and (d), as well as Figure 8, for two main reasons. First, in our previous paper [16], we found that all the moments (except for the zeroth moment) of the exit time distribution diverged when $v \ll 1$, and the error in the kth sample moment is $O(M^{-1/2}v^{-2k})$ when $v \ll 1$. For example, when v is ten times smaller, in order to keep the same magnitude of error for the first moment (i.e., mean), the amount of noisy data needs to be one hundred times larger. For fixed M, the noisy data generated from simulation becomes much less accurate when v gets smaller. Second, given $F(x) = O(1)$, $x \in [-L/2, L/2]$, it
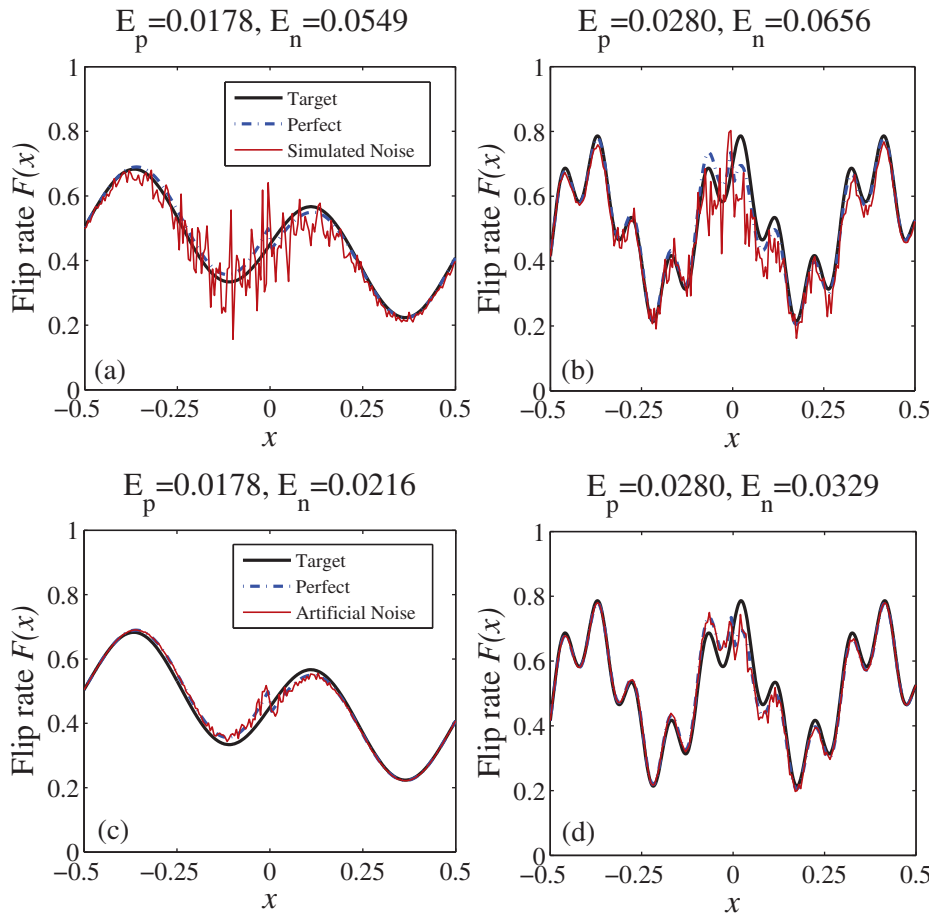
FIG. 7. *Reconstruction of flip rate functions $F(x)$ with small velocity from Monte Carlo simulation data and artificial noisy data:* (a) *and* (c) $F(x) = 0.3 \sin(5x) \cos(8x) + 0.3 \cos(0.3x) \exp(0.5x) + 0.3x^2 \sin(-0.6x^3) + 0.15$; (b) *and* (d) $F(x) = 0.5 + 0.2 \cos(16x) + 0.1 \sin(64x)$, $N = 200$, $v = 0.1$. (a) *and* (b) *are reconstructed from simulated noisy data with* $M = 1,000,000$. (c) *and* (d) *are reconstructed from artificial noisy data with* $\varepsilon = 10^{-5}$.

takes a longer time to generate data at a given accuracy when v is smaller. Specifically, let $w_{1p}(-L/2, t)$, $w_{2p}(L/2, t)$, and $w_{1n}(-L/2, t)$, $w_{2n}(L/2, t)$ for $t \in (0, L/v]$ be PDFs obtained from perfect data and Monte Carlo simulation, respectively. The PDFs $w_{1n}(-L/2, t_j)$ and $w_{2n}(L/2, t_j)$, where $t_j, j = 0, 1, \ldots, N$, are defined in section 3.2 and can be computed as follows. Suppose the two sets of M exit times are $\{\tau_k^{(1)}\}$ and $\{\tau_k^{(2)}\}$, $1 \le k \le M$. Then let

$$w_{1n}(-L/2, t) = \frac{m}{M \Delta t} \quad \text{if } t_{j-1} \le t < t_j,$$

where $\Delta t = t_j - t_{j-1}$, m is the number of exit times satisfying $t_{j-1} \le \tau_k^{(1)} < t_j$ for $1 \le j \le N$, and $w_{2n}(L/2, t)$ can be computed similarly. Define the magnitude of noise in $w_{1n}(-L/2, t)$ and $w_{2n}(L/2, t)$ by

$$\varepsilon_1 = \max_{t \in (0, L/v]} |w_{1n}(-L/2, t) - w_{1p}(-L/2, t)|, \quad \varepsilon_2 = \max_{t \in (0, L/v]} |w_{2n}(L/2, t) - w_{2p}(L/2, t)|,$$
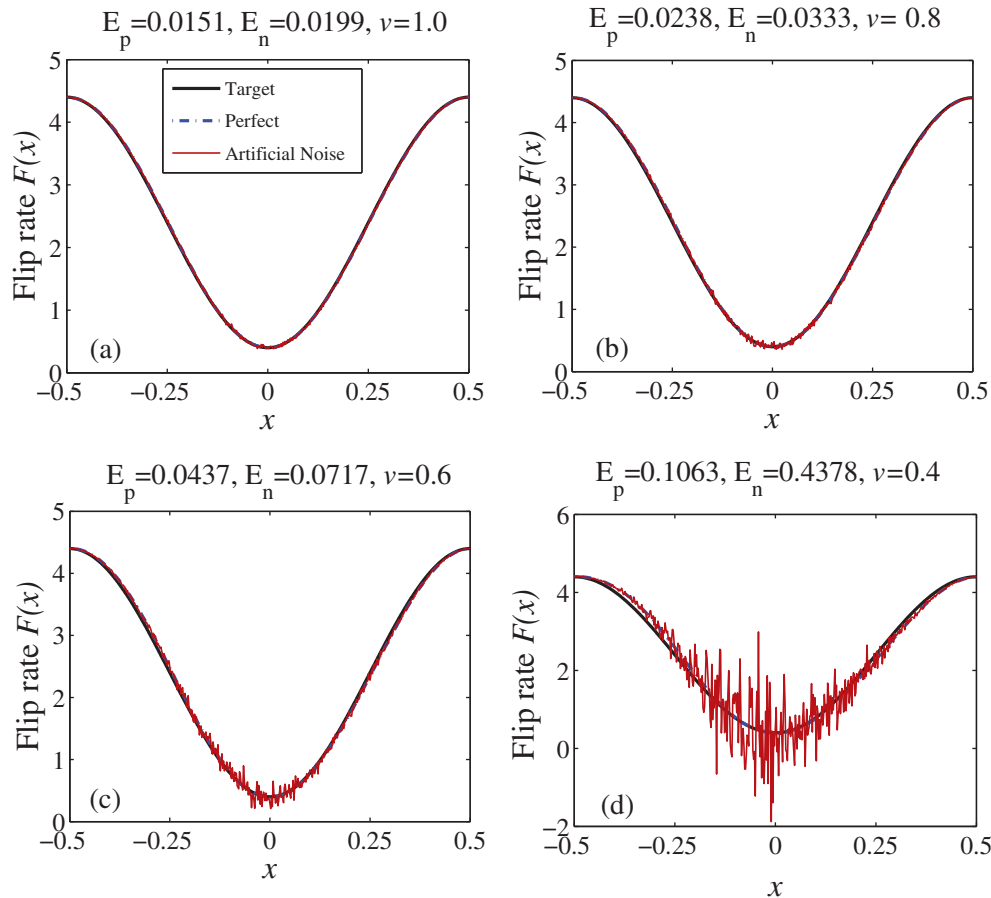
FIG. 8. *Reconstruction of flip rate functions $F(x) = -2\cos(2\pi x) + 2.4$ with different velocities from artificial noisy data: (a) $v = 1$, (b) $v = 0.8$, (c) $v = 0.6$, (d) $v = 0.4$. $F(x)$ are reconstructed from artificial noisy data with $\varepsilon = 10^{-3}$.*

respectively. For the data used to generate Figures 7(a) and (b), we find that both ε_1 and ε_2 are $O(10^{-3})$ with $N = 200$ and $2M = 2,000,000$ exit times in total, which takes more than 11 days to generate. To reduce the order of ε_1 and ε_2 to $O(10^{-5})$ (the noise level of the data in Figures 7(c) and (d)), we need to generate more exit times. However, reducing ε_1 and ε_2 to $O(10^{-5})$ would require about $2M = 4,000,000$ exit times, which would take MATLAB 22 days to complete on an AMD 2.2 GHz Opteron 6174 CPU.

5. Conclusion. In this paper, we make three contributions. First, we successfully utilize a layer stripping method, which is used by geophysicists in seismology, to study a stochastic inverse problem arising from neuroscience and medical imaging. In principle, we are able to reconstruct a wide range of continuous flip rate functions of a one-dimensional, constant-speed Broadwell process from the exit time distributions, and the error is within $O(10^{-2})$ using $2M = 400,000$ exit times in total. The reconstructed flip rate functions become less noisy, and the accuracy improves as the number of exit times increases. For instance, the reconstruction error in the L^2 norm decreases by 30%–50% when using $2M = 2,000,000$ exit times in total. Second, we

develop first order and second order layer stripping methods for flip rate reconstruction, where the second order layer stripping algorithm is developed by replacing the first order simple Euler method and rectangle rule with a predictor-corrector method and trapezoid rule. In both of the algorithms, we do not find the value of $F(x)$ at $x = 0$; so it leaves a "hole" in the $F(x)$, which is filled by interpolation. However, the second order finite difference method is second order accurate only when the boundary data is noiseless and corresponds to an actual flip rate function; otherwise, it is only first order accurate. Third, we are able to reconstruct the flip rate function $F(x)$ from noisy (artificial and Monte Carlo simulated) data when v is small, which is the important limit corresponding to a Brownian random walk.

When we reconstruct the flip rate function $F(x)$ from simulated noisy data for small v, we usually have larger deviation near $x = 0$, because the PDFs of the boundary data become less accurate when v gets smaller. To reduce the noise in the PDFs, we can increase the number of exit times, which turns out to be time consuming. The difficulty in data generation and the noise in PDFs explains the difficulties in reconstructing flip rate function for small velocity.

The layer stripping algorithm is more powerful than the projection method used in our previous paper [16] regarding the underlying mathematics and conditions for the method to be applicable. The layer stripping algorithm relies on the hyperbolicity structure of the PDE, while the projection method reconstructs the flip rate function by minimizing an objective function. Optimization can be used for all inverse problems, but usually leads to ill-posed problems. As for the conditions, the layer stripping method can, in principle, reconstruct any continuous or discontinuous flip rate function that is bounded on the finite interval of interest. In contrast, the projection method requires that the flip rate function is known to be a low-degree polynomial; this is a severe restriction. However, the layer stripping algorithm can only reconstruct flip rate functions from boundary data generated by starting a Broadwell process from either endpoint of the interval, while the projection method can reconstruct from data generated by starting a Broadwell process from any position strictly within the interval.

A sequence of studies [5, 17] shows that inverse problems associated with diffusive motions are often ill-posed, and the related existence and uniqueness of the spatially dependent parameters are not generally well-established. However, in this paper, we showed numerically that for fixed $0 < v < \infty$, reconstruction of a bounded flip rate function $F(x)$ using the Broadwell process as the underlying random walk *is* well-posed and unique. Well-posedness of the layer-stripping method is theoretically predicated on the work of Symes [32], who proved global uniqueness and stability of the method for the one-dimensional variable-coefficient acoustic wave equation. Because of the results in this paper, together with those in [32], we advocate solving first passage time inverse problems by including persistence or "memory" effects in the underlying physics governing the random walk.

In the future, we will consider smoothing the noisy simulation data by filtering so that we can retain the accuracy of the second order method. We will also apply the layer stripping method to a Broadwell process of two advection velocities $v_1(x)$ and $-v_2(x)$, as well as develop advanced numerical methods based on the layer stripping method to study Broadwell process when v is close to zero. Furthermore, we would consider using layer stripping algorithm to reconstruct a Broadwell process where one boundary (say, $-L/2$) is reflecting, the other one ($L/2$) is the absorbing exit boundary, and the particle starts at $-L/2$.

Appendix A. Derivation of the Kolmogorov backward equation for a two-state Broadwell process. We now derive the backward equation from the forward Kolmogorov equations of the Broadwell process, where the particle transits between two states: state 1 represents right-going with velocity $+v$, and state 2 represents left-going with velocity $-v$. We define x, l, and τ as the initial position, state and time, and y, k, and σ as the current position, state and time, where $l, k \in \{1, 2\}$, $x, y \in (-L/2, L/2)$. $P_{kl}(y, \sigma|x, \tau)dy$ is the probability that the particle lies in the interval $(y, y + dy)$ in state k at time σ, given that the particle initially starts at x in state l at time τ.

Consider the forward Kolmogorov equations for $P_{1l}(y, \sigma|x, \tau)$ and $P_{2l}(y, \sigma|x, \tau)$:

(A.1) $$\frac{\partial P_{1l}(y, \sigma|x, \tau)}{\partial \sigma} = -v\frac{\partial P_{1l}(y, \sigma|x, \tau)}{\partial y} + F(y)(P_{2l}(y, \sigma|x, \tau) - P_{1l}(y, \sigma|x, \tau)),$$

(A.2) $$\frac{\partial P_{2l}(y, \sigma|x, \tau)}{\partial \sigma} = v\frac{\partial P_{2l}(y, \sigma|x, \tau)}{\partial y} + F(y)(P_{1l}(y, \sigma|x, \tau) - P_{2l}(y, \sigma|x, \tau)),$$

$$P_{1l}(-L/2, \sigma|x, \tau) = 0,$$
$$P_{2l}(L/2, \sigma|x, \tau) = 0$$

for $\sigma > \tau$, and

$$P_{1l}(y, \sigma|x, \tau) = \delta_{1l}\delta(y - x),$$
$$P_{2l}(y, \sigma|x, \tau) = \delta_{2l}\delta(y - x)$$

for $\sigma \leq \tau$, where δ_{1l} and δ_{2l} are Kronecker delta functions.

We rewrite (A.1) and (A.2) in operator form as

$$\frac{\partial}{\partial \sigma}P_{kl}(y, \sigma|x, \tau) = \mathcal{L}(y, k)P_{kl}(y, \sigma|x, \tau), \quad k = 1, 2,$$

where

$$\mathcal{L}(y, k)P_{kl}(y, \sigma|x, \tau) = \sum_{k'=1}^{2} L_{kk'}(y)P_{k'l}(y, \sigma|x, \tau),$$

$$L_{11}(y) = -v\frac{\partial}{\partial y} - F(y), \quad L_{12}(y) = F(y),$$

$$L_{21}(y) = F(y), \qquad\qquad L_{22}(y) = v\frac{\partial}{\partial y} - F(y).$$

The backward equation is given in terms of the adjoint operator $\mathcal{L}^*$[2, 16] operating on the initial position and state:

$$-\frac{\partial}{\partial \tau}P_{kl}(y, \sigma|x, \tau) = \mathcal{L}^*(x, l)P_{kl}(y, \sigma|x, \tau), \quad l = 1, 2,$$

where

$$\mathcal{L}^*(x, l)P_{kl}(y, \sigma|x, \tau) = \sum_{l'=1}^{2} L_{ll'}^*(x)P_{kl'}(y, \sigma|x, \tau),$$

$$L_{11}^*(x) = v\frac{\partial}{\partial x} - F(x), \quad L_{12}^*(x) = F(x),$$

$$L_{21}^*(x) = F(x), \qquad\qquad L_{22}^*(x) = -v\frac{\partial}{\partial x} - F(x).$$

Let $t = \sigma - \tau$. Because the Broadwell process is a time homogeneous process, we have $P_{kl}(y, t|x, 0) = P_{kl}(y, \sigma|x, \tau)$ and $-\frac{\partial}{\partial \tau} = \frac{\partial}{\partial t}$. Hence, the backward equations become

$$(A.3) \qquad \frac{\partial}{\partial t} P_{k1}(y, t|x, 0) = [v\partial_x - F(x)]P_{k1}(y, t|x, 0) + F(x)P_{k2}(y, t|x, 0),$$

$$\frac{\partial}{\partial t} P_{k2}(y, t|x, 0) = F(x)P_{k1}(y, t|x, 0) + [-v\partial_x - F(x)]P_{k2}(y, t|x, 0),$$

$$P_{k1}(y, t|L/2, 0) = 0,$$
$$(A.4) \qquad P_{k2}(y, t| - L/2, 0) = 0$$

for $t > 0$, and

$$P_{k1}(y, t|x, 0) = \delta_{k1}\delta(y - x),$$
$$P_{k2}(y, t|x, 0) = \delta_{k2}\delta(y - x)$$

for $t \leq 0$. Let $S_1(x, t)$ be the probability that the particle is in $[-L/2, L/2)$ at time t given that it starts at position x in state 1, and $S_2(x, t)$ be the probability that the particle is in $(-L/2, L/2]$ at time t given that it starts at position x in state 2. Then the survival probabilities are given by

$$(A.5) \qquad S_i(x, t) = \int_{-\frac{L}{2}}^{\frac{L}{2}} \sum_{k=1}^{2} P_{ki}(y, t|x, 0)\, \mathrm{d}y, \quad i = 1, 2.$$

Substituting (A.3)–(A.4) into (A.5) gives

$$(A.6) \qquad \frac{\partial S_1}{\partial t} - v(x)\frac{\partial S_1}{\partial x} = F(x)(S_2 - S_1),$$
$$\frac{\partial S_2}{\partial t} + v(x)\frac{\partial S_2}{\partial x} = F(x)(S_1 - S_2),$$
$$S_1(L/2, t) = 0,$$
$$S_2(-L/2, t) = 0$$

for $t > 0$, and

$$S_1(x, t) = 1,$$
$$(A.7) \qquad S_2(x, t) = 1$$

for $t \leq 0$.

In fact, we observe that $S_1(L/2, t) = S_2(-L/2, t) = H(-t)$ for any t. Let $w_i(x, t), i = 1, 2$ be exit time distribution. Then we have

$$w_i(x, t)\mathrm{d}t = S_i(x, t) - S_i(x, t + \mathrm{d}t),$$
$$\Rightarrow w_i(x, t) = -\frac{\partial S_i}{\partial t}.$$

Then, taking the derivative of (A.6)–(A.7) with respect to t, we obtain (2.1)–(2.6).

Appendix B. Derivation of (3.9)–(3.10). We now show that from

$$(B.1) \qquad a_0\delta'(\xi) = 0,$$

we can derive (3.9)–(3.10). (Recall that a_0 is continuous and differentiable.) We first represent a_0 in terms of characteristic variables $\xi = t - x/v - L/2/v$ and $\eta =$

$t + x/v - L/2/v$ so that $a_0(x, t) = f(\xi, \eta)$ for some function f. Define the inner product $\langle \alpha, \beta \rangle = \int \alpha(\xi)\beta(\xi) \, d\xi$. Then (B.1) implies that for all test functions $\phi(\xi)$,

$$\langle a_0(x, t)\delta'(\xi), \phi(\xi) \rangle = 0,$$
$$\Rightarrow \langle \, \delta'(\xi), f(\xi, \eta)\phi(\xi) \, \rangle = 0,$$
$$\Rightarrow -\langle \, \delta(\xi), \partial_\xi[f(\xi, \eta)\phi(\xi)] \, \rangle = 0,$$
$$\Rightarrow -\left(f_\xi(\xi, \eta)\phi(\xi)\Big|_{\xi=0} + f(\xi, \eta)\phi'(\xi)\Big|_{\xi=0} \right) = 0.$$

Taking $\phi(\xi) \equiv 1$, we find $f_\xi(0, \eta) = 0$. Taking $\phi(\xi) = \xi\psi(\xi)$ with $\psi(0) \neq 0$, we have $f(0, \eta) = 0$. Since $\partial_\xi = \partial_t - v\partial_x$, we find that

$$a_0(x, t) = 0,$$
$$\frac{\partial a_0}{\partial t} - v\frac{\partial a_0}{\partial x} = 0$$

on $\xi = t - x/v - L/2/v = 0$.

Appendix C. Perfect exit time distribution generation. In this section, we numerically solve the forward problem (3.1)–(3.4) to generate the exit time distribution (perfect data) $w_1(-L/2, t)$, $w_2(L/2, t)$. From (3.23)–(3.24), we know that the exit time distributions are then given by

(C.1)
$$w_1(-L/2, t) = c_0(-L/2, t)\delta(t - L/v) + a_1(-L/2, t)H(t) + \widetilde{c}_1(L/2, t)H(t - L/v),$$

(C.2)
$$w_2(L/2, t) = b_0(L/2, t)\delta(t - L/v) + b_1(L/2, t)H(t - L/v) + \widetilde{d}_1(-L/2, t)H(t).$$

Because from Figure 3, we see that the values of $w_1(-L/2, t)$ at $t = L/(2v)$ and $w_2(L/2, t)$ at $t = L/(2v)$ only affect $F(x)$ at $x = 0$, a set of zero measure. Whether the delta functions are included in (C.1)–(C.2) will only affect $F(x)$ at a single point; we ignore the deltas and only need to solve for a_1, b_1, $\widetilde{c}_1$, and $\widetilde{d}_1$.

Now we describe the algorithm for solving a_1, b_1. Rewrite (3.12)–(3.14) as

(C.3) $$\frac{da_1}{dt} = F(x)(b_1 - a_1) \quad \text{on } t + x/v = \text{constant},$$

(C.4) $$\frac{db_1}{dt} = F(x)(a_1 - b_1) \quad \text{on } t - x/v = \text{constant},$$

(C.5) $$a_1(x, t) = \frac{F(x)}{2} \exp\left[-\int_{-L/2}^{x} \frac{F(x')}{v} dx' \right] \quad \text{on } t = x/v + L/(2v),$$

(C.6) $$b_1(-L/2, t) = 0.$$

Let $\Delta x = L/N, x_0 = -L/2, x_N = L/2, t_0 = 0, t_N = L/v, a_1^{(j,i)} = a_1(x_j, t_i), b_1^{(j,i)} = b_1(x_j, t_i)$, and then follow the procedure and Figure 9 below to calculate a_1 and b_1:

1. From (C.5) and (C.6), we know that a_1 (cross) is known on the diagonal $t = x/v + L/(2v)$, and b_1 (circle) is known on the left boundary $x = -L/2$. Rewrite (C.3) and (C.4) as

    (C.7) $$b_1^{(j,i)} = \Delta t F_{j-1}\left[a_1^{(j-1,i-1)} - b_1^{(j-1,i-1)} \right] + b_1^{(j-1,i-1)},$$

    (C.8) $$a_1^{(j,i)} = \Delta t F_{j+1}\left[b_1^{(j+1,i-1)} - a_1^{(j+1,i-1)} \right] + a_1^{(j+1,i-1)},$$

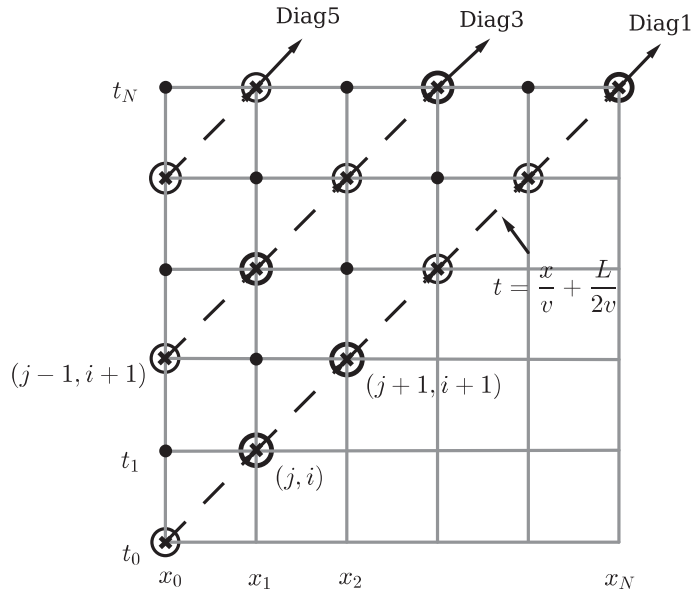   from which the value of b_1 along Diag1 $t = x/v + L/(2v)$ is updated.

FIG. 9. *Finite difference stencils for forward problem* (3.12)–(3.14). a_1 *is known on the diagonal* $t = x/v + L/(2v)$, *and* b_1 *is known on the left boundary* $x = -L/2$.

2. Use (C.8) and (C.7) to update the values of a_1 and b_1 along Diag3.

3. Repeat the previous steps to update a_1 and b_1 along every other diagonal.

4. Use linear interpolation to calculate a_1 and b_1 along Diag2, Diag4, ..., etc.
From 3.1.1, we know that $\widetilde{c}_1$ and $\widetilde{d}_1$ can be solved through (3.21)–(3.22) using the same algorithm as (3.12)–(3.14), but using $F(-x)$ instead of $F(x)$. Hence, the solution to the full forward problem (2.1)–(2.6) is constructed by solving (C.3)–(C.4) numerically.

Acknowledgments. Both QH and PWF thank Rakesh for helpful discussions.

REFERENCES

[1] Z. S. Agranovich, V. A. Marchenko, and B. D. Seckler, *The Inverse Problem of Scattering Theory*, Gordon and Breach, New York, 1963.
[2] L. J. S. Allen, *An Introduction to Stochastic Processes with Applications to Biology*, Prentice-Hall, Englewood Cliffs, NJ, 2003.
[3] S. R. Arridge, *Optical tomography in medical imaging*, Inverse Problems, 15 (1999), pp. R41–R93.
[4] S. Asmussen and P. W. Glynn, *Stochastic Simulation: Algorithms and Analysis*, Springer, New York, 2007.
[5] G. Bal and T. Chou, *On the reconstruction of diffusions from first-exit time distributions*, Inverse Problems, 20 (2004), p. 1053.
[6] D. J. Bicout, *Green's functions and first passage time distributions for dynamic instability of microtubules*, Phys. Rev. E, 56 (1997), 6656.
[7] J. E. Broadwell, *Shock structure in a simple discrete velocity gas*, Phys. Fluids, 7 (1964), pp. 1243–1247.
[8] J. E. Broadwell, *Study of rarefied shear flow by the discrete velocity method*, J. Fluid Mech., 19 (1964), pp. 401–414.
[9] A. M. Bruckstein and T. Kailath, *Inverse scattering for discrete transmission-line models*, SIAM Rev., 29 (1987), pp. 359–389.
[10] K. P. Bube and R. Burridge, *The one-dimensional inverse problem of reflection seismology*, SIAM Rev., 25 (1983), pp. 497–559.

[11] R. Burridge, *The Gelfand–Levitan, the Marchenko, and the Gopinath–Sondhi integral equations of inverse scattering theory, regarded in the context of inverse impulse-response problems*, Wave Motion, 2 (1980), pp. 305–323.

[12] A. J. Christlieb, J. A. Rossmanith, and P. Smereka, *The Broadwell model in a thin channel*, Commun. Math. Sci., 2 (2004), pp. 443–476.

[13] P. Degond and S. Motsch, *Continuum limit of self-driven particles with orientation interaction*, Math. Models Methods Appl. Sci., 18 (2008), p. 1193–1215.

[14] P. W. Fok and T. Chou, *Reconstruction of potential energy profiles from multiple rupture time distributions*, Proc. R. Soc. A Math. Phys. Eng. Sci., 466 (2010), pp. 3479–3499.

[15] P.-W. Fok, C.-L. Guo, and T. Chou, *Charge-transport-mediated recruitment of DNA repair enzymes*, J. Chem. Phys., 129 (2008), 235101.

[16] P. W. Fok, Q. Han, and T. Chou, *Reconstruction of a persistent random walk from exit time distributions*, IMA J. Appl. Math. (2013).

[17] P.-W. Fok, *Drift reconstruction from first passage time data using the Levenberg Marquardt method*, Inverse Probl. Sci. Eng., (2013), pp. 1–22.

[18] I. M. Gelfand and B. M. Levitan, *On the Determination of a Differential Equation from Its Spectral Function*, AMS, Providence, RI, 1955.

[19] W. Gerstner and W. M. Kistler, *Spiking Neuron Models: Single Neurons, Populations, Plasticity*, Cambridge University Press, Cambridge, 2002.

[20] G. M. L. Gladwell, *Inverse Problems in Scattering: An Introduction*, Springer, New York, 1993.

[21] S. Goldstein, *On diffusion by discontinuous movements, and on the telegraph equation*, Quart. J. Mech. Appl. Math., 4 (1951), pp. 129–156.

[22] B. Gopinath and M. M. Sondhi, *Determination of the shape of the human vocal tract from acoustical measurements*, Bell Syst. Tech. J., 49 (1970), pp. 1195–1214.

[23] B. Gopinath and M. M. Sondhi, *Inversion of the telegraph equation and the synthesis of nonuniform lines*, Proc. IEEE, 59 (1971), pp. 383–392.

[24] T. Kailath, B. Levy, L. Ljung, and M. Morf, *The factorization and representation of operators in the algebra generated by Toeplitz operators*, SIAM J. Appl. Math., 37 (1979), pp. 467–484.

[25] M. G. Krein, *On a method for the effective solution of the inverse boundary value problem*, Dok. Akad. Nauk SSSR, 94 (1954), pp. 987–990.

[26] J. Masoliver and G. H. Weiss, *Telegrapher's equation with variable propagation speeds*, Phys. Rev. E, 49 (1994), pp. 3852–3854.

[27] V. Rajani, G. Carrero, D. E. Golan, G. de Vries, and C. W. Cairo, *Analysis of molecular diffusion by first-passage time variance identifies the size of confinement zones*, Biophys. J., 100 (2011), pp. 1463–1472.

[28] S. Redner, *A Guide to First-Passage Processes*, Cambridge University Press, Cambridge, 2001.

[29] J. Rissanen, *Algorithms for triangular decomposition of block Hankel and Toeplitz matrices with application to factoring positive matrix polynomials*, Math. Comp., 27 (1973), pp. 147–154.

[30] F. Santosa and H. Schwetlick, *The inversion of acoustical impedance profile by methods of characteristics*, Wave Motion, 4 (1982), pp. 99–110.

[31] M. M. Sondhi and J. R. Resnick, *The inverse problem for the vocal tract: Numerical methods, acoustical experiments, and speech synthesis*, J. Acoustical Soc. Amer., 73 (1983), pp. 985–1002.

[32] W. W. Symes, *On the relation between coefficient and boundary values for solutions of webster's horn equation*, SIAM J. Math. Anal., 17 (1986), p. 1400–1420.

[33] H. C. Tuckwell, R. Rodriguez, and F. Y. M. Wan, *Determination of firing times for the stochastic Fitzhugh–Nagumo neuronal model*, Neural Comput., 15 (2003), pp. 143–159.

[34] H. C. Tuckwell, *Stochastic Processes in the Neurosciences*, Vol. 56, SIAM, Philadelphia, 1989.

[35] C. Xue and H. G. Othmer, *Multiscale models of taxis-driven patterning in bacterial populations*, SIAM J. Appl. Math., 70 (2009), pp. 133–167.